DETERMINATION OF FILTRATION CHARACTERISTICS OF POWER-LAW NON-NEWTONIAN FLUIDS–SOLIDS MIXTURES UNDER CONSTANT-PRESSURE CONDITIONS

TOSHIRO MURASE, EIJI IRITANI, JUN HYUNG CHO AND MOMPEI SHIRATO

Department of Chemical Engineering, Nagoya University, Nagoya 464

Key Words: Solid Liquid Separation, Filtration, Non Newtonian Fluid, Power Law Fluid, Constant Pressure Filtration, Filtration Area, Specific Filtration Resistance, Porosity, Compression Permeability Cell, Newtonian Fluid

Filtration characteristics of power-law non-Newtonian fluids-solids mixtures are investigated by use of a specially designed filter having a hole at the top of the filter chamber. On the basis of the principle of sudden reduction in filtration area of the cake surface, a method is developed for determining such overall filtration characteristics as the ratio m of wet to dry cake mass and the average specific filtration resistance γ_{av} for power-law fluids. Analytical equations are derived for correlating the overall filtration characteristics with the point or local values in filter cake. The compression-permeability characteristics, which are essential to the theoretical analysis of the mechanism of filtration within compressible filter cake, are evaluated on the basis of the overall filtration characteristics obtained under various filtration pressure conditions. It is shown that the results obtained from the newly developed non-Newtonian filtration technique are in good agreement with those obtained from conventional C-P (compression-permeability) cell measurements and Newtonian filtration experiments.

Introduction

Filtration of non-Newtonian fluids–solids mixtures has become increasingly important in such widely divergent fields as the petrochemical and food processing industries. In recent years, the flow mechanism of filtration of power-law fluids–solids mixtures has been analyzed in view of the flow of non-Newtonian fluids through granular beds.[6-8] In previous papers,[9,11,19-21] a more accurate non-Newtonian filtration theory applicable to compressible cake materials has been developed in consideration of the distributions of porosity and hydraulic pressure in cakes for evaluating the characteristics of both unidimensional and non-unidimensional filtration under constant-pressure, constant-rate and variable-pressure–variable-rate conditions. Both overall filtration characteristics and internal structures of the filter cake can be reasonably analyzed on the basis of experimental data of the equilibrium porosity and the specific flow resistance of the compressed cake in the C-P (compression-permeability) cell.[1-4,13,16,18] However, this technique may be rather tedious and time-consuming for industrial practice. It would be desirable to develop simple and precise test methods based on constant-pressure filtration experiments with non-Newtonian fluids.

Received May 2, 1988. Correspondence concerning this article should be addressed to T. Murase. M. Shirato is at Nagoya Industrial Science Research Institute, Nagoya 468.

In the previous paper,[10] accurate values of the ratio m of wet to dry cake mass and the average specific filtration resistance α_{av} of filter cake were determined from actual filtration experiments with Newtonian fluids, using a filter having a hole at the top of the filter chamber, on the basis of the sudden reduction in filtration area of the cake surface. Based on the experimental data relating m and α_{av} to the filtration pressure, a method has been developed for determining the local porosity ε and the local specific filtration resistance α as functions of the local solid compressive pressure p_s.

In this paper, the analytical equations derived in the previous paper[10] are modified and a simple method based upon constant-pressure filtration experiments is presented for the determination of the filtration characteristics of non-Newtonian fluids. The filtration characteristic values obtained by the newly developed method are compared with experimental data of both the conventional C-P cell measurements and filtration of Newtonian fluids.

1. Experimental Apparatus and Procedure

The experimental apparatus is essentially the same as employed in the previous study.[10] The heights h of the filter chamber range from 1 to 3 cm. A disk with a hole having a diameter D_h of 1.2 cm is placed on top of an inserted cylinder with an inner diameter D of 4 cm. The ratio of the area of the hole to the medium

area is 0.09. Non-Newtonian fluids used in this study are 0.35 wt% sodium polyacrylate–deionized water solutions, which can be treated as typical power-law fluids over the whole range of shear rates that may be encountered in these experiments. Hyflo Super-Cel is added to the polymer solutions with a solid concentration of 0.15 by weight. After the slurry is poured into the filter, constant-pressure filtration experiments are carried out by applying air pressures of 49 to 392 kPa, and the variations of filtrate volume with time are measured.

The same filtration experiments are conducted for the slurry prepared by suspending Hyflo Super-Cel in glycerin, which can be treated as Newtonian fluid. Compression-permeability tests are also conducted, using a slurry of Hyflo Super-Cel–deionized water mixture.

2. Overall Characteristics of Non-Newtonian Filter Cake

Filter cake steadily grows parallel to the filter medium as illustrated in **Fig. 1(a)** as soon as the filtration starts. The power-law model for the filtrate flow is represented by

$$\tau = K\dot{\gamma}^N \tag{1}$$

and the filtration rate u_1 can be written as[19]

$$\left(\frac{d\theta}{dv}\right)^N \equiv \left(\frac{1}{u_1}\right)^N = \frac{K\gamma_{av}\rho s}{p(1-ms)}(v+v_m) \tag{2}$$

where τ is the shear stress, K the fluid consistency index, $\dot{\gamma}$ the shear rate, N the flow behavior index, θ the filtration time, v the filtrate volume per unit medium area, γ_{av} the average specific filtration resistance for power-law fluids, ρ the density of the liquid, s the mass fraction of solids in slurry, p the applied filtration pressure, and v_m the fictitious filtrate volume per unit area. The ratio m of wet to dry cake mass is related to the thickness L of the filter cake and the filtrate volume v in the form[10]

$$m = \frac{\rho_s sv + \rho_s L - \rho sv}{\rho_s s(v+L)} = 1 + \frac{\rho\varepsilon_{av}}{\rho_s(1-\varepsilon_{av})} \tag{3}$$

where ρ_s is the true density of solids, and ε_{av} the average porosity. Such overall filtration characteristics as m and γ_{av} can be determined from the calculations based upon constant-pressure filtration data by Eqs. (2) and (3).

After the filter cake builds up to the underside of the disk, the subsequent filter cake forms only inside the hole in the disk and the surface area of the cake drops suddenly from the area of the medium to the area of the hole as indicated in **Fig. 1(b)**. Consequently, the filtrate flows only through the portion of cake under the hole. The sudden change of filtration area causes a decrease in the filtration rate.

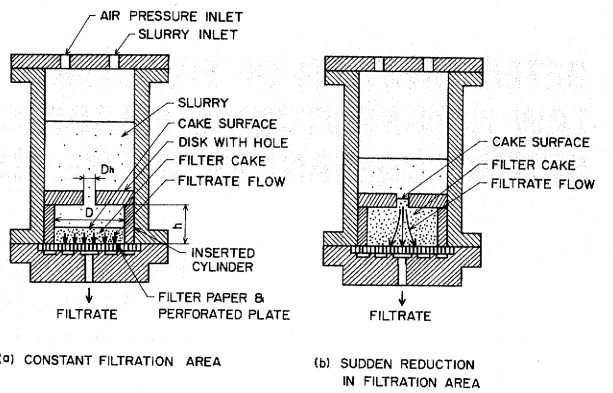

Fig. 1. Mechanism of measurement of filtration characteristics

Thus, the relation between $(d\theta/dv)^N$ vs. v deviates markedly from that represented by Eq. (2). The filtrate volume v_c at the transition point being known, the value of m can be calculated by using h in place of L as the cake thickness and v_c as v in Eq. (3). The value of γ_{av} can be obtained from Eq. (2) by using both the value of the slope in the first stage of $(d\theta/dv)^N$ vs. v and m-value.

3. Local Values of Filtration Characteristics

The filtration characteristics of local specific filtration resistance (γ for power-law fluids, α for Newtonian fluids) and local porosity ε are essential to the analytical investigation of local cake conditions as controlling the overall filtration behavior. Knowing the experimental data of γ_{av} and m vs. p, one can determine the values of γ, α and ε as mentioned below.

The average specific resistance γ_{av} for power-law fluids is generally represented in the form[19,20]

$$\gamma_{av} = \int_0^1 \left(\frac{u}{u_1}\right) d\left(\frac{\omega}{\omega_0}\right) \frac{p-p_m}{\displaystyle\int_0^{p-p_m} \frac{1}{\gamma}\, dp_s} \tag{4}$$

where u is the apparent liquid velocity relative to solids, ω the net solid volume per unit medium area lying from the medium up to an arbitrary position in the cake, ω_0 the net solid volume of the entire cake per unit medium area, and p_m the local hydraulic pressure on the medium surface. The local specific resistance γ for power-law fluids is defined by[19,20]

$$\gamma = \left\{\frac{1+\xi N}{(1+\xi)N}\right\}^N \left\{\frac{T\varepsilon^2}{kS_0(1-\varepsilon)}\right\}^{1-N} \alpha \tag{5}$$

$$\alpha = \frac{kS_0^2(1-\varepsilon)}{\rho_s\varepsilon^3} \tag{6}$$

where ξ is a geometric constant that depends upon the cross-sectional shape of the flow path,[5] T the tortuosity, k Kozeny's constant, S_0 the effective specific surface of solids, and α the local specific filtration resistance which is conventionally used for

Newtonian fluids. On the assumption that the flow rate u can be approximately regarded as constant through the entire cake and that p_m is negligible, Eq. (4) reduces to

$$\gamma_{av}=\frac{p}{\int_0^p \frac{1}{\gamma}dp_s} \tag{7}$$

Differentiating Eq. (7) with respect to p, one gets

$$\gamma=\frac{\gamma_{av}}{1-\frac{d(\ln\gamma_{av})}{d(\ln p)}} \tag{8}$$

Equation (8) can be used to relate γ to p_s on the basis of the empirical relationship between γ_{av} and p. For practical purposes, it may be possible for γ to be approximately evaluated by use of a power function.

The γ, α and ε-values depend upon the local solid compressive pressure p_s within filter cake. To relate α and ε to p_s by means of empirical formulas, the following power functions have been utilized for moderately compressible solids.[22-24]

$$\alpha=\alpha_1 p_s^n \tag{9}$$

$$\varepsilon=Ep_s^{-\lambda} \tag{10}$$

$$1-\varepsilon=Bp_s^{\beta} \tag{11}$$

where α_1, n, E, λ, B and β are empirical constants. While it may not seem consistent to represent both ε and $(1-\varepsilon)$ as different power functions of p_s, the relatively small variations in porosity permit the data to be accurately rectified by Eqs. (10) and (11). Substituting Eqs. (9)–(11) into Eq. (5), one gets

$$\gamma=\gamma_1 p_s^l \tag{12}$$

where

$$\gamma_1=\left\{\frac{1+\xi N}{(1+\xi)N}\right\}^N\left(\frac{T^2E}{k\rho_s B}\right)^{(1-N)/2}\alpha_1^{(1+N)/2} \tag{13}$$

$$l=\frac{1}{2}\{(n+\lambda+\beta)N+(n-\lambda-\beta)\} \tag{14}$$

Below some low pressure p_i the value of γ is assumed constant. On the assumption that p_i is negligible, substitution of Eq. (12) into Eq. (7) leads to

$$\gamma_{av}=\gamma_1(1-l)p^l \tag{15}$$

The values of γ_1 and l can be determined from a logarithmic plot of γ_{av} vs. p in accordance with Eq. (15).

Formulas for porosity calculations depend upon the basic flow equation for power-law fluids through compressible porous media, which is given by[19,20]

$$u^N=-\frac{1}{K\rho_s\gamma(1-\varepsilon)}\cdot\frac{dp_s}{dx} \tag{16}$$

where x is the distance from the medium. If L is the cake thickness, the average porosity ε_{av} of the cake is defined by

$$\varepsilon_{av}\equiv\frac{1}{L}\int_0^L \varepsilon dx=\frac{1}{L}\int_p^0 \varepsilon\frac{dx}{dp_s}dp_s \tag{17}$$

The derivative (dx/dp_s) can be obtained from Eq. (16) and substituted in Eq. (17) to yield

$$\varepsilon_{av}=\frac{1}{K\rho_s L}\int_0^p \frac{\varepsilon}{\gamma(1-\varepsilon)u^N}dp_s \tag{18}$$

If the local flow rate u is approximately uniform through the filter cake, the filter cake thickness can be given in the form of

$$L=\left[\int_0^p dp_s\Big/\{\gamma(1-\varepsilon)u^N\}\right]\Big/(K\rho_s)$$

from integration of Eq. (16) and substituted in Eq. (18) to yield

$$\varepsilon_{av}=1-\frac{\int_0^p \frac{dp_s}{\gamma}}{\int_0^p \frac{dp_s}{\gamma(1-\varepsilon)}} \tag{19}$$

Differentiating Eq. (19) with respect to p and rearranging with the aid of Eq. (8), the generalized equation for evaluating ε as a function of p_s is derived in the form

$$\frac{\varepsilon-\varepsilon_{av}}{1-\varepsilon}=\frac{\frac{d\{\ln(1-\varepsilon_{av})\}}{d(\ln p)}}{\frac{d(\ln\gamma_{av})}{d(\ln p)}-1} \tag{20}$$

For practical purposes, it may be convenient to utilize the power function approximation for relating $(1-\varepsilon_{av})$ to p. Substituting Eqs. (11) and (12) into Eq. (19), one gets

$$1-\varepsilon_{av}=\frac{B(1-l-\beta)}{1-l}p^{\beta} \tag{21}$$

The values of β and $B(1-l-\beta)/(1-l)$ in Eq. (21) can be empirically determined from a plot of $\ln(1-\varepsilon_{av})$ vs. $\ln p$, and B can be evaluated by use of the predetermined value of l. Thus, the relation of ε vs. p_s can be calculated by Eq. (11), and from its logarithmic plot the values of E and λ in Eq. (10) can be determined graphically. The parameters α_1 and n in Eq. (9), which are used for calculating the local specific resistance α of Newtonian filter cake, can be also obtained from Eqs. (13) and (14).

4. Experimental Results and Discussion

The flow curves of filtrate, which were determined by a cone-and-plate viscometer, are shown in **Fig. 2**. The non-Newtonian fluids used in this study exhibit

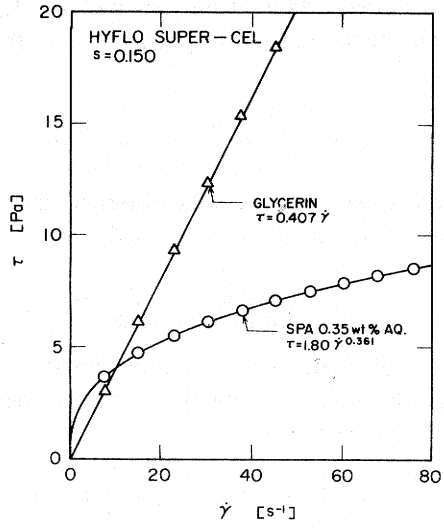

Fig. 2. Flow curves of filtrate

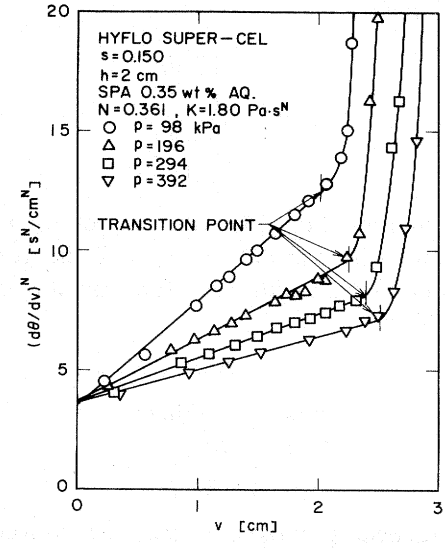

Fig. 3. Relation between $(d\theta/dv)^N$ and v

strong characteristics of pseudoplastic fluids.

The experimental values of $(d\theta/dv)^N$ are plotted against v with p as the parameter in **Fig. 3**. The filtration data yield straight lines in accordance with Eq. (2) until the cake surface reaches the underside of the disk. But after the filtrate volume v is beyond the critical volume v_c and the filter cake surface decreases suddenly, the value of $d\theta/dv$ increases abruptly. The values of m and ε_{av} can be calculated by substituting the values of both the thickness h of the filter chamber and the critical filtrate volume v_c at the transition point into Eq. (3). The γ_{av}-value can be calculated from Eq. (2) by using the m-value thus obtained.

In **Fig. 4**, $(1-\varepsilon_{av})$ is plotted against p logarithmically. The linear relation can be obtained in accordance with Eq. (21). In **Fig. 5**, where a logarithmic plot of γ_{av} vs. p is illustrated, it can be seen that γ_{av} varies approximately as a power function of p in accordance with Eq. (15). The experimental results

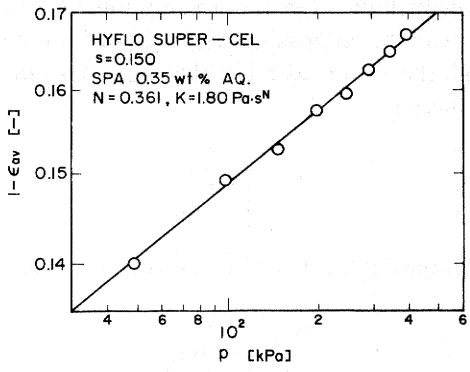

Fig. 4. Logarithmic plots of $(1-\varepsilon_{av})$ vs. p

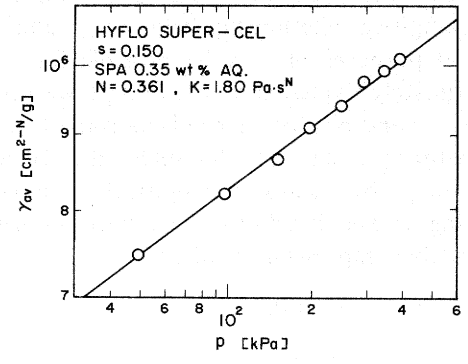

Fig. 5. Logarithmic plots of γ_{av} vs. p

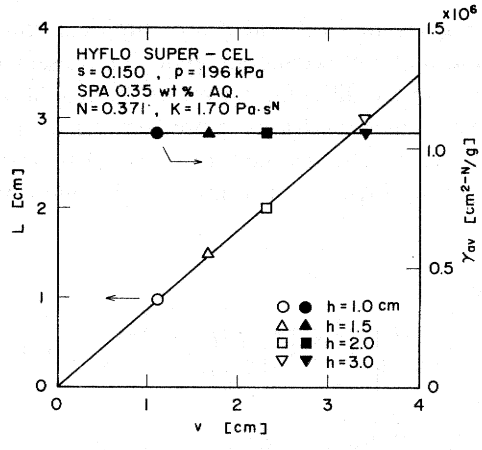

Fig. 6. Effects of v on L and γ_{av}

obtained at various heights h of the filter chamber are plotted in the form of L and γ_{av} vs. v in **Fig. 6**. It is apparent that m or ε_{av} remains constant irrespective of L in view of the linearity of L vs. v.[12,17] It is also clearly indicated that γ_{av} remains almost constant during the course of a constant-pressure filtration. Therefore, it should be noted that the measurements of m and γ_{av} are hardly affected by the height h of the first filter chamber.

In **Fig. 7**, the solid line represents the ε-values calculated by Eq. (10) on the basis of filtration experiments with non-Newtonian fluids. For comparison, the compression data obtained by C-P cell measurements and the values based upon conven-

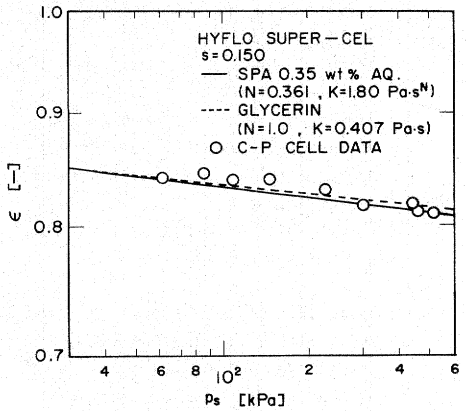

Fig. 7. Logarithmic plots of ε vs. p_s

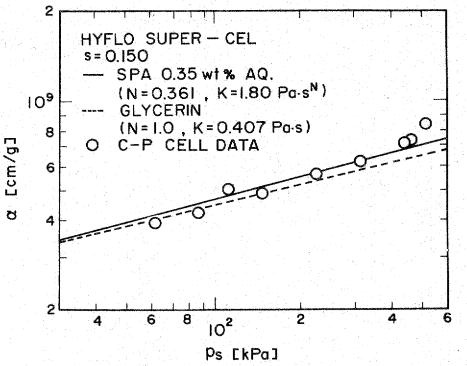

Fig. 8. Logarithmic plots of α vs. p_s

tional Newtonian filtration experiments are included. The calculated values compare favorably with the compression data. In **Fig. 8**, the permeability data of Newtonian fluid through the compressed cake in C-P cell measurements are plotted in the form of α vs. p_s. The values predicted by Eq. (9) on the basis of non-Newtonian filtration experiments are fairly consistent with both the permeability data and the filtration data of Newtonian fluid. The porosity ε and the specific filtration resistance α for the compressed cake are not influenced by the flow behavior of the filtrate, but depend only upon the property of the solid materials which constitute the cake. Thus, it is considered that the measurements based upon the non-Newtonian and Newtonian filtration experiments favorably coincide with the C-P cell data.

On the basis of the characteristic values of ε and α obtained from non-Newtonian filtration, theoretical hydraulic pressure distributions in non-Newtonian filter cake are shown in **Fig. 9**. The solid line in the figure represents the rigorous calculations, which take the variation of the flow rate into account, obtained by[20]

$$\frac{p_L}{p}=\frac{\int_0^{\omega/\omega_0}\left(\frac{u}{u_1}\right)^N \gamma d\left(\frac{\omega}{\omega_0}\right)}{\int_0^1\left(\frac{u}{u_1}\right)^N \gamma d\left(\frac{\omega}{\omega_0}\right)} \tag{22}$$

or

$$1-\frac{\int_0^{p_s}\frac{dp_s}{\gamma}}{\int_0^{p}\frac{dp_s}{\gamma}}=\frac{\int_0^{\omega/\omega_0}\left(\frac{u}{u_1}\right)^N d\left(\frac{\omega}{\omega_0}\right)}{\int_0^1\left(\frac{u}{u_1}\right)^N d\left(\frac{\omega}{\omega_0}\right)} \tag{23}$$

where p_L is the local hydraulic pressure. The broken line represents the calculations based upon the following relation, which is derived by substituting Eq. (12) into Eq. (23) on the assumption that the flow rate u is kept constant.

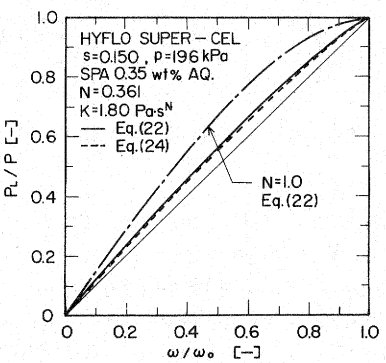

Fig. 9. Hydraulic pressure distributions in cake

$$\frac{p_L}{p}=1-\left(1-\frac{\omega}{\omega_0}\right)^{1/(1-l)} \tag{24}$$

From the fact that both calculations yield quite close values, it is considered that the approximation of the constant flow rate may be valid in the determination of compression-permeability characteristics from the experimental results of non-Newtonian filtration. The dot-dash-line and the diagonal line in the figure denote the hydraulic pressure distributions in Newtonian filter cake and incompressible cake, respectively. The figure indicates that hydraulic pressure in cake decreases with decreasing N and this results in lower-porosity cake as previously reported.[19]

To verify the validity of the compression-permeability characteristics obtained from non-Newtonian filtration experiments, the predicted values based upon these data are compared with experimental results for Newtonian filtration.[14,15] The reciprocal flow rate $d\theta/dv$ is plotted against v in **Fig. 10**. The solid line represents the values calculated by setting N as unity, γ_{av} as α_{av} and K as the viscosity μ of Newtonians in Eq. (2).

Conclusion

Filtration experiments of power-law non-Newtonian fluids–solids mixtures were conducted under constant-pressure conditions, using a test filter equipped with a disk having a hole on top of the filter chamber. The ratio m of wet to dry cake mass and the

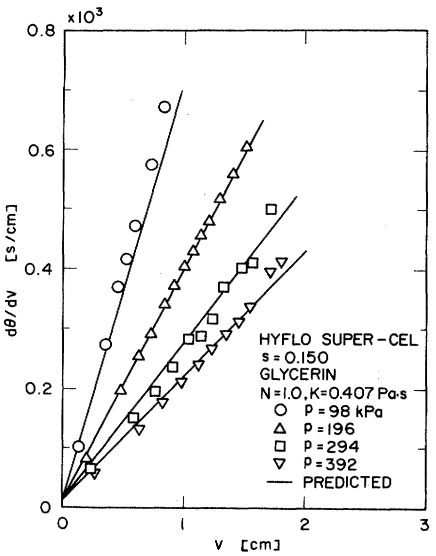

Fig. 10. Relation between $d\theta/dv$ and v for Newtonian filtration

average specific filtration resistance γ_{av} of non-Newtonian filter cake were evaluated on the basis of the principle of sudden reduction in filtration area of the cake surface. By using m and γ_{av} obtained under various filtration pressures, a method has been developed for determining local values such as ε and α as functions of p_s. The filtration characteristic values nearly coincided with those based upon both Newtonian filtration experiments and C-P cell measurements.

Acknowledgment

This work was supported by the Ministry of Education, Japan (Special Research Project on Environmental Science, Grant No. 61030031 and Encouragement of Research, Grant No. 62750852), and by the Asahi Glass Foundation for Industrial Technology, Tokyo, Japan. The authors acknowledge with gratitude the financial support leading to the publication of this article.

Nomenclature

B	=	constant defined in Eq. (11)	$[kg^{-\beta}m^{\beta}s^{2\beta}]$
D	=	inner diameter of inserted cylinder	[m]
D_h	=	diameter of hole	[m]
E	=	constant defined in Eq. (10)	$[kg^{\lambda}m^{-\lambda}s^{-2\lambda}]$
h	=	height of filter chamber	[m]
K	=	fluid consistency index	$[Pa\cdot s^{N}]$
k	=	Kozeny's constant	[—]
L	=	cake thickness	[m]
l	=	constant defined by Eq. (14)	[—]
m	=	ratio of wet to dry cake mass	[—]
N	=	flow behavior index	[—]
n	=	exponent defined by Eq. (9)	[—]
p	=	applied filtration pressure	[Pa]
p_i	=	low pressure below which porosity and specific resistance are constant	[Pa]
p_L	=	local hydraulic pressure	[Pa]
p_m	=	local hydraulic pressure on medium surface	[Pa]
p_s	=	local solid compressive pressure	[Pa]
S_0	=	effective specific surface of solids	$[m^{-1}]$
s	=	mass fraction of solids in slurry	[—]
T	=	tortuosity factor	[—]
u	=	apparent liquid velocity relative to solids	[m/s]
u_1	=	filtration velocity	[m/s]
v	=	filtrate volume per unit medium area	[m]
v_c	=	filtrate volume per unit medium area collected until cake surface reaches disk with hole	[m]
v_m	=	fictitious filtrate volume per unit area	[m]
x	=	distance from medium	[m]
α	=	local specific filtration resistance for Newtonian fluid defined by Eq. (6)	[m/kg]
α_1	=	constant defined in Eq. (9)	$[kg^{-1-n}m^{1+n}s^{2n}]$
α_{av}	=	average specific filtration resistance for Newtonian fluid	[m/kg]
β	=	exponent defined by Eq. (11)	[—]
γ	=	local specific filtration resistance for power-law fluid defined by Eq. (5)	$[m^{2-N}/kg]$
γ_1	=	constant defined by Eq. (13)	$[kg^{-1-l}m^{2-N+l}s^{2l}]$
γ_{av}	=	average specific filtration resistance for power-law fluid defined by Eq. (4)	$[m^{2-N}/kg]$
$\dot{\gamma}$	=	shear rate	$[s^{-1}]$
ε	=	local porosity	[—]
ε_{av}	=	average porosity defined by Eq. (17)	[—]
θ	=	filtration time	[s]
λ	=	exponent defined by Eq. (10)	[—]
μ	=	viscosity of Newtonian fluid	[Pa·s]
ξ	=	geometric constant depending on cross-sectional shape of flow path	[—]
ρ	=	density of liquid	$[kg/m^3]$
ρ_s	=	true density of solids	$[kg/m^3]$
τ	=	shear stress	[Pa]
ω	=	net solid volume per unit medium area lying from medium up to an arbitrary position in cake	[m]
ω_0	=	net solid volume of entire cake per unit medium area	[m]

Literature Cited

1) Carman, P. C.: *Trans. Instn. Chem. Engrs. (London)*, **16**, 168 (1938).
2) Carman, P. C.: *J. Soc. Chem. Ind.*, **58**, 1 (1939).
3) Grace, H. P.: *Chem. Eng. Progr.*, **49**, 303 (1953).
4) Grace, H. P.: *Chem. Eng. Progr.*, **49**, 367 (1953).
5) Kozicki, W., C. J. Hsu and C. Tiu: *Chem. Eng. Sci.*, **22**, 487 (1967).
6) Kozicki, W., C. Tiu and A. R. K. Rao: *Can. J. Chem. Eng.*, **46**, 313 (1968).
7) Kozicki, W., A. R. K. Rao and C. Tiu: *Chem. Eng. Sci.*, **27**, 615 (1972).
8) Kozicki, W.: Proc. of World Congress III of Chem. Eng., Vol. III, Japan, p. 134 (1986).
9) Murase, T., K. Kobayashi, E. Iritani, K. Ito and M. Shirato: *J. Chem. Eng. Japan*, **18**, 230 (1985).
10) Murase, T., E. Iritani, J. H. Cho, S. Nakanomori and M. Shirato: *J. Chem. Eng. Japan*, **20**, 246 (1987).
11) Murase, T., E. Iritani, M. Hattori, K. Kobayashi and M. Shirato: *J. Chem. Eng. Japan*, **20**, 632 (1987).
12) Okamura, S. and M. Shirato: *Kagaku Kōgaku*, **19**, 104 (1955).
13) Okamura, S. and M. Shirato: *Kagaku Kōgaku*, **19**, 111 (1955).
14) Ruth, B. F.: *Ind. Eng. Chem.*, **25**, 153 (1933).
15) Ruth, B. F.: *Ind. Eng. Chem.*, **27**, 806 (1935).
16) Ruth, B. F.: *Ind. Eng. Chem.*, **38**, 564 (1946).
17) Shirato, M., T. Murase, H. Kato and S. Fukaya: *Kagaku Kōgaku*, **31**, 1125 (1967).

18) Shirato, M., T. Aragaki, R. Mori and K. Sawamoto: *J. Chem. Eng. Japan*, **1**, 86 (1968).
19) Shirato, M., T. Aragaki, E. Iritani, M. Wakimoto, S. Fujiyoshi and S. Nanda: *J. Chem. Eng. Japan*, **10**, 54 (1977).
20) Shirato, M., T. Aragaki and E. Iritani: *J. Chem. Eng. Japan*, **13**, 61 (1980).
21) Shirato, M., T. Aragaki, E. Iritani and T. Funahashi: *J. Chem. Eng. Japan*, **13**, 473 (1980).
22) Tiller, F. M.: *Chem. Eng. Progr.*, **49**, 467 (1953).
23) Tiller, F. M.: *Chem. Eng. Progr.*, **51**, 282 (1955).
24) Tiller, F. M. and C. J. Huang: *Ind. Eng. Chem.*, **53**, 529 (1961).

(Presented at the 53rd Annual Meeting of The Society of Chemical Engineers, Japan, at Sendai, April, 1988.)